# The Guanine Tautomer Puzzle: Quantum Chemical Investigation of Ground and Excited States

**Christel M. Marian**[†]

*Institute of Theoretical and Computational Chemistry, Heinrich-Heine-University Düsseldorf, 40225 Düsseldorf, Germany*

*Received: December 15, 2006*

Combined density functional and multireference configuration interaction methods have been employed to explore the ground and low-lying electronically excited states of the most important tautomeric and rotameric forms of guanine with the purpose of resolving the conflicting assignments of IR−UV bands found in the literature. The calculations predict sharp $^1(\pi\rightarrow\pi^*)$ origin transitions for the $RN_1$ rotamer of the 7H-amino-hydroxy species and the $RN_7$ rotamer of the 9H-amino-hydroxy species. The other 9H-amino-hydroxy rotamer, $RN_1$, undergoes ultrafast nonradiative decay and is thus missing in the UV spectra. Because of its very small Franck−Condon factor and the presence of a conical intersection close by, it appears questionable, whether the $^1(\pi\rightarrow\pi^*)$ origin transition of 9H-amino-oxo-guanine can be observed experimentally. Vibrational overlap is more favorable for the $^1(\pi\rightarrow\pi^*)$ origin transition of the 7H- amino-oxo form, but also this tautomer is predicted to undergo ultrafast nonradiative decay of the $^1(\pi\rightarrow\pi^*)$ population. The good agreement of calculated IR frequencies of the amino-oxo species with recent IR spectra in He droplets and their mismatch with peaks observed in IR−UV spectra indicate that none of the bands stem from 7H- or 9H-amino-oxo guanine. Instead, our results suggest that these bands originate from 7H-imino-oxo guanine tautomers. In the excited-state dynamics of the biologically relevant 9H-amino-oxo tautomer, a diffuse charge transfer state is predicted to play a significant role.

## I. Introduction

Excited-state lifetimes of nucleic acid bases and the nucleosides are short in solution and in the gas phase.[1] Exponential decay times in the sub-picosecond range were determined for photoexcited guanine by gas-phase femtosecond pump−probe spectroscopy.[2,3] However, guanine exists in several low-energetic tautomeric forms with overlapping UV spectra, which cannot be distinguished by this technique. The biologically relevant form of guanine is the 9H-1H-amino-oxo (9H-1H-AO-G) tautomer (see Chart 1). Knowledge of its response to photoexcitation by UV light is therefore particularly important.

In principle, double-resonance optical spectroscopy is capable of providing tautomer-specific information.[4,5,6,7,8,9] The presence or absence of fundamental O−H and N−$H_2$ stretching modes in IR−UV double resonance spectra allows to differentiate between amino-oxo (AO), amino-hydroxy (AH), imino-oxo (IO), and imino-hydroxy (IH) forms of guanine. So far, two different AH species with origins at 32864 $cm^{-1}$ (A) and 34755 $cm^{-1}$ (D) were identified in molecular beams, whereas the bands with origins at 33269 $cm^{-1}$ (B) and 33910 $cm^{-1}$ (C) were assigned to AO forms.[5,7−9] In addition, a few weak bands at the low-frequency side of the A origin were observed (A′) and tentatively assigned to originate from the same species as the A band.[6] In contrast to adenine, the 9H and 7H tautomers of guanine cannot be distinguished by IR−UV double resonance spectroscopy because their ground-state vibrational frequencies are too similar. The assignment of a UV band system to a particular tautomer was therefore based on the comparison with spectra of methylated species.[7,8] Typically, methylation of a purine base causes a small red shift of the $S_1$ origin but does not change the essential characteristics of a band. This relation holds true for the AH forms and has led to the assignments of the A band to 7H-AH-G and of the D band to 9H-AH-G, but

**CHART 1: Chemical Structures of the Eight Most Stable Tautomeric and Rotameric Forms of Guanine in the Gas Phase: 1, 9H-1H-AO-G; 2, 7H-1H-AO-G; 3, 9H-AH-G ($RN_1$); 4, 9H-AH-G ($RN_7$); 5, 7H-AH-G ($RN_1$); 6, 7H-3H-AO-G; 7, 7H-1H-3H-IO-G (Z); 8, 7H-1H-3H-IO-G (E)**

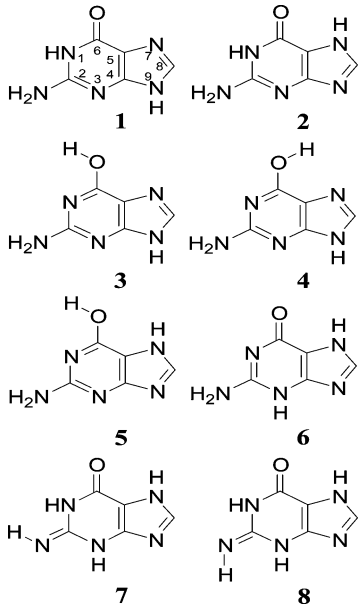


[†] To whom correspondence should be addressed. Phone: +49 211 8113209. Fax: +49 211 8113466. E-mail: Christel.Marian@uni-duesseldorf.de.

10.1021/jp068620v CCC: $37.00 
Published on Web 02/03/2007

this does not appear to be the case for the 9H/9Me-1H-AO forms. Resonant two-photon ionization (R2PI) spectra of 9Me-1H-AO-G[5,7,10] and guanosine[11] have not been observed, whereas the band systems B and C of guanine (assigned to 9H-1H-AO-G by Nir et al.[5,8] and Mons et al.,[7] respectively) exhibit discrete features in IR-labeled R2PI spectroscopy and clear origin transitions in dispersed fluorescence spectra.[9]

Very recently, 9H-1H-AO-G, 7H-1H-AO-G, and two rotamers of 9H-AH-G were identified by the orientation of their transition dipole moment angles in an IR laser spectroscopic study of guanine in helium droplets.[12] Unfortunately, the IR bands observed in the latter study and in the IR−UV molecular beam experiments do not overlap particularly well, the discrepancies being stunningly large for the asymmetric $NH_2$ stretching modes of 9H-1H-AO-G and 7H-1H-AO-G.[12] To resolve the guanine tautomer puzzle, further information on the ground and electronically excited states of the guanine tautomers is required. The quantum chemical investigation presented in this work sheds light on their electronic and nuclear structures. It does not only give clues about the identity of the tautomers but explains why other tautomers are missing in the IR−UV and R2PI spectra. For other purine bases, the theoretical methods applied here yielded results sufficiently accurate to aid the assignment of experimental bands and to provide insight in the details of nonradiative relaxation mechanisms after electronic excitation.[13,14] Parallel to the present theoretical study, quantum chemical investigations were conducted in other laboratories.[15−17] The reassignment of the IR−UV spectrum of guanine proposed by these authors is consistent with the conclusions drawn here.

## II. Theoretical Methods

Ground-state geometries, harmonic vibrational frequencies, and ionization potentials were determined at the restricted Kohn−Sham level (B3-LYP functional),[18,19,20] utilizing the Turbomole quantum chemistry program package.[21] For the eight most stable guanine tautomers, geometry optimizations of the excited singlet states were carried out at the level of time-dependent density functional theory (TDDFT).[22] Harmonic vibrational frequencies of the first excited$^1(\pi\rightarrow\pi^*)$ states were evaluated numerically using the SNF package.[23] Zero-point vibrational energy (ZPVE) corrections were scaled by 0.9613.[24] At the optimized ground- and excited-state geometries, single-point calculations were carried out employing the combined density functional theory/multireference configuration interaction (DFT/MRCI) method by Grimme and Waletzke.[25] In the MRCI step, all valence electrons were correlated, and twelve roots of singlet multiplicity were determined simultaneously.

Harmonic vibrational frequencies were obtained using TZVP (valence triple-$\zeta$ plus (d,p) polarization) basis sets from the Turbomole library.[26] For all other properties, the atomic orbital basis was augmented by two sets of diffuse basis functions with exponents taken from recent work on adenine.[13] The Rydberg functions were located at dummy centers, the positions of which were allowed to vary freely in the geometry optimization step. Auxiliary basis functions for the resolution-of-the-identity approximation of two-electron integrals in the MRCI calculations were taken from the Turbomole library.[27] Molecular structures and orbitals have been visualized using Molden.[28]

## III. Results and Discussion

**A. Tautomer Stabilities and IR Frequencies.** In principle, guanine exhibits 15 tautomeric forms, some of which may exist in multiple conformations. There is consensus that guanine has four low-energetic tautomers in the gas phase, i.e., 9H-1H-AO-G, 9H-AH-G, 7H-1H-AO-G, and 7H-AH-G.[29,30,31,32] However, under laser-desorption conditions, also less favorable tautomeric species can be populated to a minor extent. A quick scan at the DFT level of theory showed that the IH forms correspond to high-energetic minima on the ground state potential energy landscape, but the 7H-3H-AO-G tautomer (with hydrogen attached to $N_3$ instead of $N_1$) and the Z and E conformations of the 7H-1H-3H-IO-G tautomer turned out to be promising candidates.

In the AH tautomers, two rotameric forms exist, $RN_1$ and $RN_7$. The rotamers differ in the orientation of the O−H bond, which points toward the $N_1$ and $N_7$ centers, respectively. Both positions correspond to minima on the ground-state potential energy hypersurface (PEH). While the $RN_1$ and $RN_7$ rotamers of 9H-AH-G are nearly isoenergetic, steric hindrance due to the $N_7$−H bond places the $RN_7$ minimum of 7H-AH-G about 3000 $cm^{-1}$ above the $RN_1$ rotamer. The 7H-AH-G ($RN_7$) rotamer is therefore not considered further.

The calculated relative stabilities and scaled harmonic vibrational frequencies of the eight most stable tautomeric and rotameric forms are listed in Table 1 together with corresponding experimental IR frequencies. The isolated 9H-1H-AO-G and 7H-1H-AO-G tautomers and the two 9H-AH rotamers $RN_7$ and $RN_1$ are so close in energy that their order depends on the theoretical method and basis set used. At the most advanced level of theory applied in this work (DFT/MRCI employing the TZVP + Rydberg basis), the energetically most favorable tautomer is 7H-1H-AO-G, followed by the two 9H-AH rotamers $RN_7$ and $RN_1$, and 9H-1H-AO-G. The 7H-AH-G ($RN_1$) species is somewhat less stable, in agreement with previous theoretical work.[29,30,31] Their Boltzmann population ratios (BPR), calculated for an estimated laser desorption temperature of 900 K (see Table 1), suggest that these five tautomeric forms of guanine should be present in the molecular beam in considerable quantities. For the 7H-3H-AO-G tautomer, Hanus et al.[30] report an enthalpy difference of 6.05 kcal $mol^{-1}$ (2116 $cm^{-1}$) with respect to 7H-1H-AO-G, comparable to our value of 2410 $cm^{-1}$. Imino-oxo tautomers were not studied by these authors. In principle, IO tautomers can be generated from the AO forms by H migration from the amino group to the neighboring $N_3$ center. As guanine is arranged in dimers in the solid state, another possibility is an asymmetric break-up of a guanine dimer upon laser desorption. The Z and E conformations of the 7H-1H-3H-IO-G tautomer exhibit comparable ground-state equilibrium energies. Our calculations place the Z form 2090 $cm^{-1}$ above the 7H-1H-AO-G tautomer, in qualitative agreement with a recent independent study by Shukla and Leszczynski.[16] At a typical laser-desorption temperature of 900 K, the BPRs of the 7H-3H-AO-G and 7H-1H-3H-IO-G species are of the order of a few percent only. The corresponding 9H-1H-3H-IO-G species are significantly less stable. Their minima are located roughly 5000 $cm^{-1}$ above the 9H-1H-AO-G tautomer, definitively too high to be generated in considerable quantities even at high temperatures.

The N−H vibrational frequencies of the AH tautomers in the He droplet IR[12] and the IR−UV double resonance experiments[5,7−9] are reproduced well by the calculations. The O−H stretching frequencies appear to be somewhat overestimated (10−20 $cm^{-1}$) by the scaled DFT values. With regard to the antisymmetric $NH_2$ stretching modes of the AO tautomers, the agreement between the calculated values and IR laser data in helium droplets[12] is very good. The discrepancies between these experimental results and the peak positions in the IR−UV spectra[5,7−9] of the B and C bands and the lack of the

**TABLE 1: Relative Stabilities[a] $\Delta E$ ($cm^{-1}$) and Harmonic Vibrational Frequencies[b] $\nu$ ($cm^{-1}$) of Selected Guanine Tautomers in the Electronic Ground State[c]**

| species | $\Delta E$ | BPR | N−$H_2$ sym | Im−H | $N_1$−H | $N_3$−H | $N_9$−H/$N_7$−H | N−$H_2$ anti | O−H |
|---|---|---|---|---|---|---|---|---|---|
| 9H-1H-AO | 470 | 0.47 | 3434 | | 3448 | | 3504 | 3540 | |
| | | | (59) | | (51) | | (77) | (40) | |
| IR[d] | | | [3445] | | [3438] | | [3507] | [3545] | |
| [C band][e] | | | [−] | | [3449] | | [−] | [3503][g] | |
| [B band][f] | | | [−] | | [3456] | | [3490] | [3506] | |
| 7H-1H-AO | 0 | 1.00 | 3425 | | 3447 | | 3503 | 3527 | |
| | | | (50) | | (52) | | (101) | (36) | |
| IR[d] | | | [3431] | | [3441] | | [3505] | [3527] | |
| [B band][e] | | | [−] | | [3456] | | [3504] | [−] | |
| [C band][f] | | | [−] | | [3450] | | [3497] | [3505] | |
| 9H-AH ($RN_1$) | 460 | 0.48 | 3462 | | | | 3507 | 3583 | 3598 |
| | | | (83) | | | | (82) | (45) | (91) |
| IR[d] | | | [3465] | | | | [3511] | [3581] | [3584] |
| [A band][f] | | | [3462] | | | | [3516] | [3577] | [3587] |
| 9H-AH ($RN_7$) | 400 | 0.53 | 3467 | | | | 3503 | 3591 | 3609 |
| | | | (97) | | | | (82) | (52) | (87) |
| IR[d] | | | [3466] | | | | [3510] | [3583] | [3591] |
| [D band][e,h] | | | [−] | | | | [3508] | [3583] | [3590] |
| [A band][f] | | | [3462] | | | | [3516] | [3577] | [3587] |
| 7H-AH ($RN_1$) | 980 | 0.21 | 3459 | | | | 3514 | 3579 | 3600 |
| | | | (75) | | | | (93) | (43) | (90) |
| [A band][e] | | | [3462] | | | | [3515] | [3577] | [3587] |
| 7H-1H-3H-IO (Z) | 2090 | 0.04 | | 3391 (16) | 3466 (54) | 3492 (104) | 3502 (111) | | |
| 7H-1H-3H-IO (E) | 2270 | 0.03 | | 3385 (14) | 3460 (82) | 3500 (84) | 3500 (104) | | |
| 7H-3H-AO | 2410 | 0.02 | 3426 | | | 3477 | 3497 | 3532 | |
| | | | (56) | | | (73) | (105) | (41) | |

[a] Tautomer energies include zero-point vibrational corrections. [b] Calculated vibrational frequencies are scaled by 0.9613. [c] Calculated IR intensities (km $mol^{-1}$) are displayed in parentheses, experimental frequencies that were assigned to the corresponding IR transitions are shown in brackets, Boltzmann population ratios (BPR) with respect to the 7H-1H-AO-G tautomer were calculated for a laser desorption temperature of 900 K, and for chemical structures, see Chart 1. [d] IR laser spectroscopy in He droplets, Choi and Miller.[12] [e] IR−UV spectroscopy, Mons et al.[7] [f] IR−UV spectroscopy, Nir et al.[5] [g] Tentative assignment. Alternative assignation to the $N_9$−H stretching mode. [h] Assignment to the $RN_7$ rotameric form by comparison of the spectra of 9methyl guanine and its hydrate, Chin et al.[37]

fundamental symmetric $NH_2$ stretching transitions in the IR−UV spectra make the assignment of the B and C bands to the 9H-1H-AO-G or 7H-1H-AO-G species questionable. The specific IR frequency pattern with two close-lying intense peaks in the 3500-$cm^{-1}$ region suggests the possibility that these bands might originate from 7H-1H-3H-IO-G tautomers. While the $N_7$−H stretching frequency is nearly identical in the 7H-1H-3H-IO-G (Z) and 7H-1H-AO-G, the $N_1$−H transition is slightly blue-shifted. The calculated frequency of the $N_3$−H stretching vibration falls nicely between the other two and is close to the value of 3490 $cm^{-1}$ measured by Nir et al.[5] in SHB spectra of the B band. The $N_{im}$−H fundamental transition has very low intensity and will be difficult to observe. A similar conclusion concerning the origin of the B and C bands was drawn very recently in an independent study by Mons et al.[15] It remains to be seen (section III.B) whether the electronic excitation energy of this species matches the spectral region of these bands.

In the electronic ground state, all AO and AH tautomers of guanine possess a slightly pyramidal amino group, while the purine ring and the carbonyl or enol moieties lie in a plane. The pyramidal structure of the amino group obtained at the DFT level was recently confirmed by ab initio calculations employing extended basis sets.[33] The IO tautomers exhibit planar equilibrium nuclear arrangements in the electronic ground state.

**B. Electronic Excitation.** The marked Franck−Condon (FC) activity in the experimental R2PI spectra points toward large geometry changes upon $S_0$−$S_1$ excitation.[9] To account for relaxation effects, we optimized the nuclear arrangements in the corresponding $S_1$ $^1(\pi\rightarrow\pi^*)$ states. In addition, the minima of the lowest-lying Rydberg singlet states ($^1A''$) were determined as these were found to play an important role in the photophysics of 9H-1H-AO-G.

Vertical and adiabatic $^1(\pi\rightarrow\pi^*)$ excitation energies of the eight most favorable tautomeric and rotameric forms, the energies and FC factors of their origin transitions, electric dipole oscillator strengths, and ionization potentials at the neutral ground- and excited-state geometries are collected in Table 2. Within the error bars of the respective methods, the vertical DFT/MRCI absorption energies presented here agree well with the CASPT12 results by Chen and Li.[17] The TDDFT energies, on the other hand, determined by Shukla and Leszczynski[16] employing the B3-LYP functional, are systematically higher, presumably due to the use of Hartree−Fock-optimized geometries by the latter authors. Differences in the adiabatic excitation energies are more subtle and do not follow a general trend. They will be discussed separately in the context of the respective tautomer.

*9H-1H-AO-G.* At the $S_0$ geometry (Figure 1a), the first excited singlet state exhibits ($\pi\rightarrow\pi^*$) character, both at the TDDFT and DFT/MRCI levels of theory. The oscillator strength for absorption is large, and the bands originating from this tautomer are thus expected to have high intensity. A singlet state with diffuse charge distribution, $^1(\pi\rightarrow$Ryd), and the $^1(n_O\rightarrow\pi_{CO}^*)$ state are located approximately 2500 $cm^{-1}$ higher in energy at this point of the coordinate space. When the nuclear geometry is relaxed on the $S_1$ PEH after vertical excitation, the minimum of the Rydberg-type state is reached (see below). To locate the $^1(\pi\rightarrow\pi^*)$ potential well, the $S_1$ geometry was pre-optimized employing the TZVP atomic orbital basis excluding diffuse functions. After convergence, Rydberg functions were added

**TABLE 2: Computed Vertical Absorption, Adiabatic, and 0−0 Excitation Energies $\Delta E$ ($cm^{-1}$) of the Lowest Singlet $\pi\rightarrow\pi^*$ States of Selected Guanine Tautomers (Dipole Oscillator Strengths $f(r)$ and Franck−Condon Factors of the Origin Transitions Are Dimensionless; Ionization Potentials at the $S_0$ and $S_1$ Geometries Are Given in Units of eV)**

| species | $\Delta E_{vert}$ | $\Delta E_{adia}$ | $\Delta E_{0-0}$ | $f(r)_{vert}$ | $FC_{0-0}$ | IP@$S_0$ | IP@$S_1$ |
|---|---|---|---|---|---|---|---|
| 9H-1H-AO | 36 530 | 32 630[a] | 32 350 | 0.22 | $<10^{-52}$ | 7.91 | 9.94 |
| 7H-1H-AO | 37 300 | 35 190[b] | 33 810 | 0.18 | $0.14\times10^{-2}$ | 8.04 | 8.11 |
| 9H-AH ($RN_1$) | 36 280 | 35 180[c] | not calcd[d] | 0.15 | | 7.89 | 8.82 |
| 9H-AH ($RN_7$) | 36 680 | 35 590 | 34 660 | 0.17 | $0.26\times10^{-5}$ | 7.90 | 8.47 |
| 7H-AH ($RN_1$) | 35 390 | 33 640 | 32 330 | 0.12 | 0.16 | 7.93 | 8.02 |
| 7H-IO (Z) | 35 914 | 33 430 | 32 160 | 0.15 | $0.63\times10^{-1}$ | 8.07 | 8.47 |
| 7H-IO (E) | 36 180 | 33 800[e] | 32 500 | 0.15 | $0.32\times10^{-1}$ | 8.13 | 8.56 |
| 7H-3H-AO | 40 480[f] | *g* | | 0.33 | | 8.33 | |

[a] Conical intersection with $S_0$ occurs approximately at 32 960 $cm^{-1}$. [b] Conical intersection with $S_0$ is located approximately at 33 280 $cm^{-1}$. [c] Electronic energy at conical intersection with $S_0$ amounts to approximately 35 730 $cm^{-1}$. [d] Minimum could not be located at the TDDFT level employing the TZVP basis set. [e] Geometry optimization of the $S_1$ state was constrained to $C_s$ symmetry. [f] Data refer to the $S_2$ state. The $S_1$ state has $^1(n\rightarrow\pi^*)$ character with $\Delta E_{vert}$ = 33 460 $cm^{-1}$. [g] See text for a rough estimate of the adiabatic excitation energy.

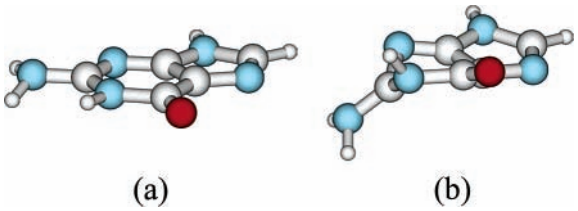


**Figure 1.** Minimum nuclear arrangements of 9H-AO-G in the $S_0$ state (a) and the $S_1$ $^1(\pi\rightarrow\pi^*)$ state (b).

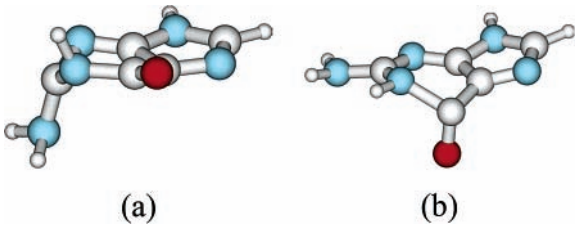


**Figure 2.** Nuclear structures of 9H-1H-AO-G at conical intersections between the $S_1$ and $S_0$ states: (a) $^1(\pi\rightarrow\pi^*)/S_0$; (b) $^1(n_O\rightarrow\pi_{CO}^*)/S_0$.

and the geometry was refined. The resulting $^1(\pi\rightarrow\pi^*)$ excited-state nuclear structure is highly distorted (Figure 1b). The puckering of the six-membered ring is accompanied by marked bond elongations, the most prominent being the elongation of the $C_2-N_3$ bond by 17 pm and of the $C_4-C_5$ bond by 8 pm. A similar minimum structure was recently determined by Chen and Li[34] at the CASSCF level of theory. Mennucci et al.[35] and Shukla and Leszczynski[32] report significantly less distorted $S_1$ geometries, but their results are based on CIS calculations that do not include major parts of electron correlation.

Our calculations place the $^1(\pi\rightarrow\pi^*)$ origin of the 9H-1H-AO-G species in the vicinity of the A band, clearly at longer wavelengths than the corresponding feature in 7H-1H-AO-G (see below). It is thus tempting to assign the B band with origin at 33 269 (refs 7 and 9) or 33 275 $cm^{-1}$ (refs 5 and 8) to the former species. However, the chances for observing the origin of the $^1(\pi\rightarrow\pi^*)$ band of 9H-1H-AO-G are very small because of various reasons. The huge geometry distortion in the electronically excited-state leads to negligibly small FC factors and a strong increase of the ionization potential (see Table 2). Furthermore, we find a conical intersection with the electronic ground state merely 330 $cm^{-1}$ above the minimum of the $^1(\pi\rightarrow\pi^*)$ state. Because of the ultrafast nonradiative decay of the excited-state population, spectral lines originating from the $^1(\pi\rightarrow\pi^*)$ transition of this tautomer will be lifetime broadened. At the conical intersection, the out-of-plane distortion of the $C_2$ center amounts to approximately 90° (Figure 2a). Similar observations were made recently by Chen and Li.[34] They determined a barrier height of 1.7 kcal $mol^{-1}$ (600 $cm^{-1}$) for the conical intersection employing CASPT2//CASSCF methods.

Another low-lying conical intersection of the $S_1$ and $S_0$ PEHs with a potential energy of approximately 34600 $cm^{-1}$ was found when searching for the minimum of the $^1(n_O\rightarrow\pi_{CO}^*)$ state. In this case, the decisive coordinate is the out-of-plane distortion of the purine ring at the $C_6$ center (Figure 2b). Similar conical intersections were reported for the $^1(n\rightarrow\pi^*)$ states of 9H-adenine,[38,40,41] where the amino group is attached to $C_6$.

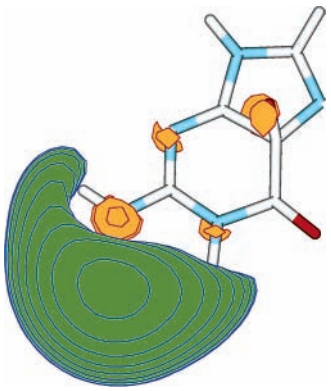

**Figure 3.** Rydberg orbital in the low-lying $^1(\pi\rightarrow Ryd)$ state of 9H-1H-AO-G.

Among the guanine tautomers, 9H-1H-AO-G is particular in the sense that it exhibits a large static dipole moment (6.8 Debye), which stabilizes diffuse, easily polarizable charge distributions. The lowest-lying Rydberg orbital (Figure 3) is of $\sigma$-type and encases the amino hydrogen atoms as well as the hydrogen atom attached to $N_1$. With respect to these N−H bonds it exhibits slightly antibonding characteristics. Because of the protruding negative charge in the vicinity of the amino group, the static dipole moment of the $^1(\pi\rightarrow Ryd)$ electronic structure (12.8 Debye) is even larger than that of the electronic ground state. Because of its charge-transfer character and its easy energetic accessibility, this state will presumably play a central role in the production of guanine ions. The planar minimum structure of $^1(\pi\rightarrow Ryd)$ with an adiabatic excitation energy of 34 760 $cm^{-1}$ corresponds to a local minimum on the $S_1$ PEH, i.e., the Rydberg state lies energetically below the $^1(\pi\rightarrow\pi^*)$ state. The band origin is located near 34 000 $cm^{-1}$,[36] well within the experimentally scanned wavelength range. However, the electronic oscillator strength of the $^1(\pi\rightarrow Ryd)$ excitation is about 30 times smaller than for the $^1(\pi\rightarrow\pi^*)$ transition. We therefore

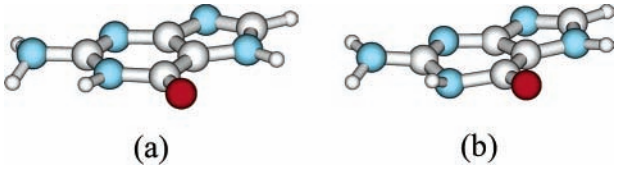


**Figure 4.** Minimum nuclear structures of 7H-1H-AO-G in the $S_0$ (a) and $S_1$ (b) states.

consider the probability for observing the direct $^1(\pi\rightarrow\text{Ryd})$ transition in absorption to be low. The picture could change in emission. FC factors are in favor of the $^1(\pi\rightarrow\text{Ryd})$ transition because the minimum nuclear structures of initial and final states are much closer here. We expect the maximum of the fluorescence from the CT state at about 31 400 $cm^{-1}$.

Another point worth mentioning is the energetic proximity of the Rydberg minimum and a planar $^1(\pi\rightarrow\pi^*)$ structure that was determined under symmetry constraints. According to our calculations, the electronic excitation energy of the latter amounts to 34 400 $cm^{-1}$. Transitions to the top of double-minimum potential for the ring-puckering mode exhibit sizable FC factors. They are thus expected to be strong and could populate the Rydberg state indirectly via vibronic coupling.

*7H-1H-AO-G.* At the DFT/MRCI level of theory, 7H-1H-AO-G (Figure 4 a) exhibits the highest vertical $^1(\pi\rightarrow\pi^*)$ absorption energy of all investigated tautomers, safe for 7H-3H-AO-G where the $^1(\pi\rightarrow\pi^*)$ excitation yields the $S_2$ state (Table 2). In contrast to the situation in adenine and 2-aminopurine, 9H to 7H tautomerization of amino-oxo guanine thus leads to a blue shift of the $^1(\pi\rightarrow\pi^*)$ excitation energy. This observation is in agreement with the results of earlier MRCI calculations by Mennucci et al.[35] employing the CIPSI method but disagrees with the trends observed in a recent TDDFT study by Shukla and Leszczynski[16,32] and CASPT2 results by Chen and Li.[17] Geometry relaxation of the $S_1$ state of 7H-1H-AO-G leads to a stabilization by more than 2000 $cm^{-1}$. The minimum nuclear geometry of the $^1(\pi\rightarrow\pi^*)$ excited-state found in the present study (Figure 4 b) is characterized by elongations of the $N_7-C_8$, $C_4-C_5$, and $N_1-C_6$ bonds and a slight puckering of the six-membered ring at the $N_1$ center. With an electronic oscillator strength of 0.18 and a FC factor of the order of $10^{-3}$, the 0−0 transition is considered to be medium strong. Chen and Li[17] obtained a significantly more distorted minimum nuclear structure at the CASSCF level of theory, similar to the one they reported for 9H-1H-AO-G. The large difference between the adiabatic CASPT2 excitation energy (3.97 eV ≈ 32 000 $cm^{-1}$) of Chen and Li and the present DFT/MRCI value of 35 190 $cm^{-1}$ is mainly due to geometric effects. The local potential well that we find in the FC region is rather flat. As a consequence, the ZPVE correction to the adiabatic excitation energy of the $^1(\pi\rightarrow\pi^*)$ state is large in this tautomer. Our calculated 0−0 transition energy of the 7H-1H-AO-G form at 33 810 $cm^{-1}$ is in excellent agreement with the experimentally observed origin of the C band at 33 910 $cm^{-1}$ (refs 7 and 9) or 33 914 $cm^{-1}$ (refs 5 and 8) and thus favors the assignment by Nir et al.[5,8] over the alternative assignment by Mons et al.[7] However, the IR−UV double resonance spectrum does not match with the calculated frequency of the asymmetric $NH_2$ stretch and the He droplet results.[12] Thus the question arises why discrete peaks of 7H-1H-AO-G have not been observed in R2PI experiments. Vertical ionization potentials of this tautomer, computed at the ground- and excited-state geometries, amount to 8.04 and 8.11 eV, respectively. They are thus well within the energy range that can be addressed by the probe laser and do not explain the lack of 7H-1H-AO-G.

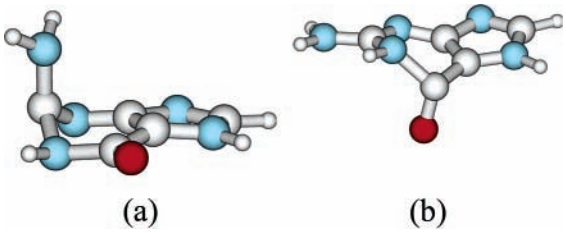


**Figure 5.** Nuclear structure of 7H-1H-AO-G at conical intersections between the $S_1$ and $S_0$ states: (a) $^1(\pi\rightarrow\pi^*)/S_0$; (b) $^1(n_O\rightarrow\pi_{CO}^*)/S_0$.

In search of a conical intersection with the $S_0$ state, a constrained minimum energy path (CMEP) along the $N_{am}-C_2-C_4-C_5$ out-of-plane coordinate was constructed. At the $^1(\pi\rightarrow\pi^*)$ minimum, this dihedral angle amounts to 165.8°. The transition state is located close to the minimum at a dihedral angle of about 160°, its energy lying marginally (60 $cm^{-1}$) above the minimum. Conical intersections between the $S_1$ and $S_0$ PEHs of the 7H-1H-AO-G form were detected for all $N_{am}-C_2-C_4-C_5$ angles smaller than 150°. The lowest point on the CMEP was found for a dihedral angle of 85° (Figure 5 a). Its adiabatic excitation energy amounts to 33 280 $cm^{-1}$ and is thus significantly lower than that of the local $^1(\pi\rightarrow\pi^*)$ minimum in the FC region. These results lead us to conclude that the 7H-1H-AO-G tautomer possesses an ultrafast relaxation pathway to the electronic ground state along the $C_2$ puckering mode, explaining its lack in the experimental UV double resonance spectra.

In an attempt to localize the minimum of the $^1(n_O\rightarrow\pi_{CO}^*)$ state, which is the second excited singlet state in the vertical absorption spectrum, another conical intersection between the $S_1$ and $S_0$ PEH was detected where the $C_6-O$ bond is almost perpendicular to the ring (Figure 5b). At the intersection, the potential energy is nearly identical with the local $^1(\pi\rightarrow\pi^*)$ minimum energy. Whether this relaxation pathway constitutes another ultrafast decay channel for photoexcited 7H-1H-AO-G molecules in the $^1(\pi\rightarrow\pi^*)$ potential energy well depends crucially on the height and width of the barrier separating these two areas of the $S_1$ PEH. An estimate of the barrier characteristics was obtained by constructing a CMEP along the $O-C_6-C_5-C_4$ coordinate. For the oxygen out-of-plane distortion the transition state is located about 1800 $cm^{-1}$ above the minimum. This decay channel will therefore play only a minor role.

The lowest-lying Rydberg state of 7H-1H-AO-G is the third excited singlet state at the $S_0$ geometry. The $^1(\pi\rightarrow\text{Ryd})$ minimum ($\Delta E_{adia}$ = 36 300 $cm^{-1}$) is located on the $S_1$ PEH, but it appears to be well separated from the $^1(\pi\rightarrow\pi^*)$ minimum. Vibronic interactions between the $^1(\pi\rightarrow\text{Ryd})$ and the $^1(\pi\rightarrow\pi^*)$ states are thus expected to be of less importance.

*9H-AH-G.* The vertical $^1(\pi\rightarrow\pi^*)$ absorption energies and oscillator strengths of the two 9H-AH-G rotamers are nearly identical. Nevertheless, the $RN_1$ and $RN_7$ forms show distinct relaxation characteristics in the excited state. A geometry optimization of the $^1(\pi\rightarrow\pi^*)$ state at the TDDFT level starting from the $S_0$ equilibrium nuclear structure of the $RN_1$ form (Figure 6 a) drives the system directly toward a conical intersection with the electronic ground state (Figure 7). The $S_1$ minimum is situated only slightly lower in energy ($\Delta E \approx 500$ $cm^{-1}$). It is found when the geometry optimization is started from the $S_1$ minimum of the $RN_7$ rotamer (see below) after having rotated the OH bond by 180°. In the minimum nuclear arrangement (Figure 6 b), the O−H group is deflected out of plane, but to a smaller extent than at the conical intersection and the purine skeleton is less distorted.

Chen and Li[17] did not perform calculations on this rotamer. Shukla and Leszczynski[16] report a calculated value for the

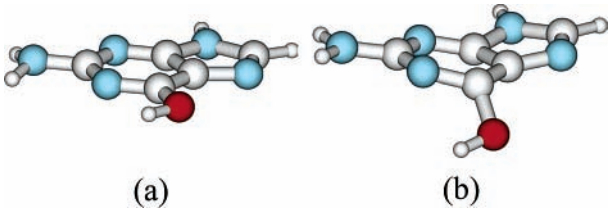


**Figure 6.** Minimum nuclear arrangements of the $RN_1$ rotamer of 9H-AH-G in the $S_0$ state (a) and in the $S_1$ $^1(\pi\rightarrow\pi^*)$ state (b).

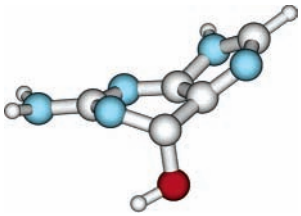

**Figure 7.** Nuclear structure of 9H-AH-G ($RN_1$) at a conical intersection between the $S_0$ and $S_1$ states close to the $^1(\pi\rightarrow\pi^*)$ minimum.

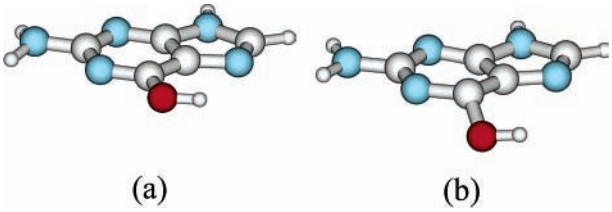


**Figure 8.** Minimum geometries of the $RN_7$ rotamer of 9H-AH-G in the $S_0$ (a) and $S_1$ (b) states.

adiabatic excitation energy of this species but have not investigated nonradiative relaxation pathways.

The ground state minimum geometry of the 9H-AH-G ($RN_7$) form is displayed in Figure 8 a. For this species, we find a $^1(\pi\rightarrow\pi^*)$ minimum nuclear structure (Figure 8 b) in which the purine rings remain essentially planar. The $C_4-C_5-C_6-O$ dihedral angle amounts to $-43°$ in this case. With respect to the ground state structure, the $C_6-O$ and $C_5-C_6$ bonds are appreciably elongated, whereas the neighboring $C_6-N_7$ bond is shortened. With a FC factor of the order of $10^{-6}$, the 0−0 transition of the $^1(\pi\rightarrow\pi^*)$ band of the $RN_7$ rotamer is expected to be rather weak but observable.

For understanding the photophysics of the 9H-AH-G species, knowledge of the barrier height for the internal rotation of the O−H bond in the electronically excited state is essential. To this end, we constructed a CMEP, beginning at the $^1(\pi\rightarrow\pi^*)$ minimum of the $RN_7$ rotamer and keeping the $C_5-C_6-O-H$ dihedral angle fixed while optimizing all other degrees of freedom. A one-dimensional cut through the PEH along this reaction coordinate is displayed in Figure 9. At the DFT/MRCI level of theory, the transition state connecting the two rotamers is situated merely 1200 $cm^{-1}$ above the $RN_7$ minimum. Tunneling through the barrier should therefore be fast. The conical intersection between the $S_0$ and $S_1$ states of the $RN_1$ rotamer is nearly isoenergetic with the minimum of the $RN_7$ rotamer. Excitation of the internal OH rotational motion will thus lead to fast nonradiative decay of 9H-AH-G.

Our calculated energetic position of the 0−0 line at 34 660 $cm^{-1}$ compares very well with the experimental origin transition of the D band[7,9] at 34 755 $cm^{-1}$ and corroborates the experimental assignment to the $RN_7$ rotameric form of 9H-AH-G.[37] Chin et al.[9] observe efficient fluorescence quenching of the D band and suggest that very effective nonradiative decay is at play in the excited state of this tautomer. In principle, this explanation is supported by our results but the details of the proposed mechanism differ. We do not find any indication of a $^1(n\rightarrow\pi^*)$ state in the vicinity of the $^1(\pi\rightarrow\pi^*)$ minimum. Instead, our calculations suggest that the fluorescence quenching of the D band is brought about by the internal rotation of the OH group in the excited state and the subsequent ultrafast nonradiative decay of the $RN_1$ rotameric form of 9H-AH-G. The easy energetic accessibility of this relaxation path also explains the lack of vibrational structure in the D band beyond 360 $cm^{-1}$ mentioned by Chin et al.[9]

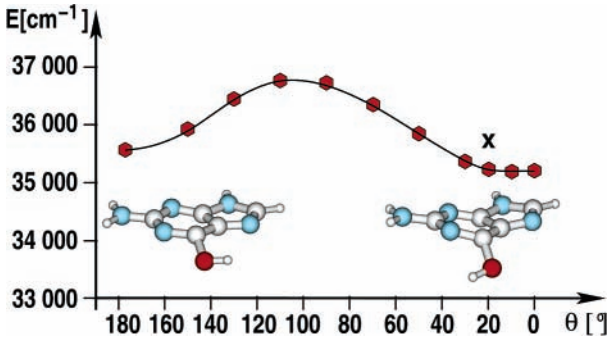


**Figure 9.** Reaction path on the $^1(\pi\rightarrow\pi^*)$ PEH of 9H-AH-G connecting the $RN_1$ (0°) and $RN_7$ (180°) rotamers. **x** indicates the energetic position of a conical intersection between the $S_0$ and $S_1$ states.

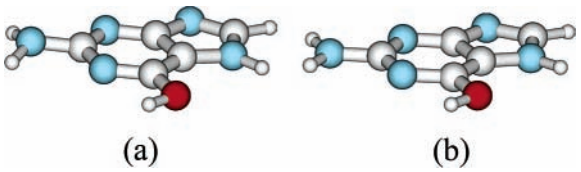


**Figure 10.** Minimum nuclear arrangements of the $RN_1$ rotamer of 7H-AH-vav G in the $S_0$ state (a) and in the $S_1$ $^1(\pi\rightarrow\pi^*)$ state (b).

The $\pi\rightarrow$Ryd excitations of the 9H-AH-G rotamers are located at markedly higher excitation energies than in the 9H-1H-AO form. The lowest-lying Rydberg-type orbital in the 9H-AH-G species has its origin near the $N_9$ center and exhibits antibonding properties with respect to the $N_9-H$ bond. The minimum of the $RN_1$ rotamer is located at 38 610 $cm^{-1}$. In the $RN_7$ rotamer, optimization of its geometric structure leads to spontaneous N−H bond dissociation. The electronic energy at conical intersection with $S_0$ amounts to roughly 36 000 $cm^{-1}$. This $^1(\pi\rightarrow\sigma^*)$ decay channel is separated from the $^1(\pi\rightarrow\pi^*)$ minimum by a considerable barrier, however. It is therefore expected to play a minor role in the low-energy photophysics of the 9H-AH-G rotamers.

*7H-AH-G.* The $RN_1$ rotamer of 7H-AH-G possesses the lowest vertical absorption energy of all investigated tautomeric and rotameric forms. We do not have a qualitative explanation why the $^1(\pi\rightarrow\pi^*)$ electronic excitation is more favorable in the 7H-AH-G tautomer compared to 9H-AH-G, while the contrary is true for the corresponding AO species. Unlike the ground-state nuclear structure (Figure 10 a), the $^1(\pi\rightarrow\pi^*)$ excited-state minimum exhibits a planar amino group (Figure 10 b). Compared to the other tautomers, the geometry shift upon $S_0-S_1$ excitation is modest. The most pronounced change is encountered in the imidazole subunit where the $N_7-C_8$ bond is elongated by 6 pm with respect to the ground state equilibrium structure and twisted by about 5°. As a consequence, it 0−0 transition has a large FC factor (0.16). The electronic transition

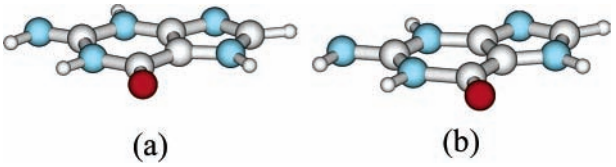


**Figure 11.** Minimum nuclear arrangements of the 7H-1H-3H-IO-G (Z) isomer in the $S_0$ state (a) and in the $S_1$ $^1(\pi\rightarrow\pi^*)$ state (b).

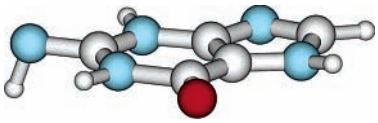

**Figure 12.** Nuclear structure of 7H-1H-3H-IO-G at the $^1(n\rightarrow\pi^*)$ minimum.

moment is somewhat smaller than for the other tautomers but still gives rise to significant oscillator strength. No conical intersections have been detected in the vicinity of the $^1(\pi\rightarrow\pi^*)$ minimum. Despite the lower stability of this tautomer in the electronic ground state and the concomitant minor abundance in the molecular beam (estimated BPR of roughly 0.2 with respect to 7H-1H-AO-G), we expect the UV bands to be strong. Diffuse states ($\Delta E_{adia} = 38\,340$ cm$^{-1}$) are of less importance in the low-energy regime photophysics of 7H-1H-AO-G.

*7H-1H-3H-IO-G*. The $S_0$ and $S_1$ states of 7H-1H-3H-IO-G (Z) exhibit planar minimum nuclear structures (parts a and b of Figure 11). Upon $^1(\pi\rightarrow\pi^*)$ excitation, the double bond between the imino nitrogen and the $C_2$ center is broken. With a length of 137 pm in the excited state, this C−N bond clearly resembles a typical amino bond. The reorganization of the electronic structure leads to significant alternate bond length changes in the purine ring, which are particularly strong in the pyrimidine subunit. The largest effect is found for the $N_1-C_6$ bond, which is elongated by 12 pm. Despite the substantial geometry changes, the FC factor for the 0−0 transition has appreciable size. If this species can be generated by laser desorption with an abundance sufficient for its detection, we expect to see a clear origin transition in the UV spectrum close to the A band origin.

The second excited singlet state in the vertical absorption spectrum of the 7H-1H-3H-IO-G species at 38 020 cm$^{-1}$ originates from a $^1(n\rightarrow\pi^*)$ configuration where the in-plane nonbonding orbital is mainly localized at the imino N. Its geometry relaxation yields a second minimum ($\Delta E_{adia} = 37\,280$ cm$^{-1}$) on the first excited singlet PEH. At this local $S_1$ minimum, the $N_{im}-H$ bond is oriented perpendicular to the purine ring (Figure 12). It thus makes no sense differentiating between Z and E conformers here. The geometry distortion in the excited-state leads to a marked rise of the ground state energy (16 880 cm$^{-1}$), which is, however, not sufficient to cause an intersection of the $S_1$ and $S_0$ PEHs. Rydberg states are supposed to play a minor role in the 7H-1H-3H-IO-G species.

In the E conformer, the $^1(\pi\rightarrow\pi^*)$ and $^1(n\rightarrow\pi^*)$ states lie closer in energy. At the $S_0$ geometry, they are separated by less than 1500 cm$^{-1}$. Unconstrained optimization leads to the $^1(n\rightarrow\pi^*)$ minimum (Figure 12). The minimum of the $^1(\pi\rightarrow\pi^*)$ state could be located at the level of TDDFT when diffuse functions were excluded from the basis set. As for the Z conformer, it has a planar nuclear structure. A refinement of the $^1(\pi\rightarrow\pi^*)$ geometry at the TDDFT (B3-LYP) level including diffuse basis functions is possible only under symmetry constraints. The complete disappearance of any barrier between the two potential wells is most likely an artifact of the TDDFT method. The preference of $^1(n\rightarrow\pi^*)$ excitations over $^1(\pi\rightarrow\pi^*)$ excitations at this level of theory has been noted earlier for 9H-adenine[13] and is considered a serious drawback of this approach used for the geometry optimization of the excited states, in particular for molecular systems like the nucleic acid bases with very close-lying excited singlet states. At the DFT/MRCI level, the adiabatic excitation energy of the E isomer is slightly higher than for the Z form, in agreement with the trends showing up in the vertical absorption spectrum and the results of recent independent theoretical studies.[16,17]

In section III.A, it had been shown that the pattern of the vibrational peaks in the B and C bands of the IR−UV spectral hole burning spectra matches well with the calculated vibrational frequencies of the two 7H-1H-3H-IO-G species. Our computed $^1(\pi\rightarrow\pi^*)$ 0−0 excitation energy of the Z form is about 1100 cm$^{-1}$ lower than the measured B band origin. Assigning the C band to the E form of 7H-1H-3H-IO-G results in a deviation of the calculated transition energy from the experimental value by about 1400 cm$^{-1}$. Deviations of this size fall well within the error bars of the DFT/MRCI method. Nevertheless it should be mentioned that the agreement between theory and experiment is significantly better for the A and D bands where the assignment is unambiguous. Similar uncertainties concerning the UV spectra of the 7H-1H-3H-IO-G isomers arise in case of the CASSCF/CASPT2 study by Chen and Li.[17] The adiabatic excitation energies, reported by these authors, are too high. They predict the $^1(\pi\rightarrow\pi^*)$ peak position in the Z form to coincide with the D band while the wave length of the E form is markedly blue shifted with respect to this band.[17] Thus, a residual tentativeness remains in the assignment of the B and C bands to a specific guanine tautomer.

*7H-3H-AO-G*. The $N_1-H/N_3-H$ tautomerization of 7H-AO-G does not only lead to a significant increase of the ground-state energy. It has severe effects on the electronic structure, too. 7H-3H-AO-G is the only guanine tautomer for which we find a $^1(n\rightarrow\pi^*)$ structure as the $S_1$ state in the vertical absorption spectrum. The optically bright $^1(\pi\rightarrow\pi^*)$ transition lies about 7000 cm$^{-1}$ higher in energy. Geometry optimizations for both states were performed without diffuse functions. From the corresponding preliminary DFT/MRCI calculations, rough estimates for the adiabatic excitation energies can be deduced, yielding values of about 30 800 cm$^{-1}$ for the $^1(n\rightarrow\pi^*)$ state and 38 200 cm$^{-1}$ for the $^1(\pi\rightarrow\pi^*)$ structures. Both transitions lie clearly outside the experimentally observed spectral range. We have therefore refrained from refining these estimates.

## IV. Summary and Conclusions

For seven of the eight investigated low-energetic tautomeric and rotameric forms of guanine, the $^1(\pi\rightarrow\pi^*)$ excitation represents the global minimum on the $S_1$ PEH, the exception being the 7H-3H-AO-G tautomer which possesses a low-lying $^1(n\rightarrow\pi^*)$ state.

According to the present theoretical investigation, the relative intensities of the UV bands of the guanine tautomers are mainly determined by FC factors, excited-state lifetimes, and the population ratios of the species in the molecular beam. Electronic dipole oscillator strengths of the $^1(\pi\rightarrow\pi^*)$ transitions and ionization potentials are of less importance for the spectral intensities. The ability to observe discrete bands for a specific tautomer/rotamer is closely related to the absence of conical intersections in the vicinity of its $^1(\pi\rightarrow\pi^*)$ minimum. Reaction coordinates leading to low-energetic conical intersections are out-of-plane distortions at the $C_2$ or $C_6$ centers of the purine ring. Ultrafast relaxation pathways of this kind are found for the biologically relevant form of guanine, 9H-1H-AO-G, for

its 7H tautomer 7H-1H-AO-G and the $RN_1$ rotamer of the 9H-AH-G species, explaining the lack of discrete bands in the UV spectra of these tautomers. Conical intersections between the $^1(\pi\rightarrow\pi^*)$ and the $S_0$ potential surfaces brought about by the strong puckering of the six-membered purine ring appear to be a common feature in purine bases. They are easily accessible in the other naturally occurring purine nucleo base, 9H-adenine, causing the ultrafast radiationless decay of the excited state.[13,38−42] In contrast, a substantial barrier has to be overcome in the fluorescent 2-aminopurine[14,42,43] and 7H-adenine.[44]

In 9H-1H-AO-G, a low-lying diffuse state has been detected on the $S_1$ PEH that plays a significant role in the photophysics of this species. Because of its charge-transfer character, we assume this state to be involved as an intermediate in the formation of guanine ions.

Comparison between available experimental data and our theoretical results leads to the following interpretation of the gas-phase guanine tautomer UV spectra:

**A Band.** Our calculations clearly support the assignment of this band to the $RN_1$ rotamer of 7H-AH-G by Mons et al.[7,9] The band origin of the $^1(\pi\rightarrow\pi^*)$ transition of 7H-AH-G (positioned at 32 330 $cm^{-1}$ in our calculations in good agreement with the measured origin of the A band at 32 864 $cm^{-1}$ (refs 7 and 9) or 32 870 $cm^{-1}$ (refs 5 and 8)) has the largest FC factor of all tautomeric forms considered in this work. Together with the respectable electric dipole oscillator strength this explains the remarkably high relative intensity of the A origin, despite of the low population of this tautomer in the molecular beam.

**B and C Bands.** By means of various double-resonance techniques, it was shown that the B and C bands do not originate from AH forms of guanine.[5,7−9] The lack of the O−H vibrational mode in the IR−UV spectra was taken as an indication that these bands stem from AO forms. Both 7H-1H-AO-G and 9H-1H-AO-G are abundant in the molecular beam but possess ultrafast nonradiative decay channels for the $^1(\pi\rightarrow\pi^*)$ population that prevent the observation of discrete IR−UV or R2PI bands. The B and C bands do therefore not stem from these AO species.

The positive assignment of the B and C bands is less certain than for the A and D bands. The pattern of the vibrational peaks in the IR−UV spectral hole burning spectra points toward another azine bond present in the molecule, as found, e.g., in an imino-oxo structure. The infrared signatures of the Z and E forms of 7H-1H-3H-IO-G, calculated in this work and in a recent publication by Mons et al.,[15] are in good agreement with the spectral hole burning patterns of the B and C bands.[5,8] Our computed $^1(\pi\rightarrow\pi^*)$ 0−0 excitation energy of the Z form is about 1100 $cm^{-1}$ lower than the measured B band origin. The transition is found to have substantial oscillator strength and a good vibrational overlap. The small population of this species in the laser desorption process could explain the relatively low intensity of the discrete peaks in the B band. The origin transition of the E form is predicted to have shorter wave length than the Z isomer and is tentatively assigned to the C band.

**D Band.** This band originates from the $^1(\pi\rightarrow\pi^*)$ excitation of the $RN_7$ rotameric form of 9H-AH-G (9H-enol (*cis*)). The calculated energetic position of the 0−0 line at 34 660 $cm^{-1}$ compares very well with the experimental origin transition of the D band[7,9] at 34 755 $cm^{-1}$. According to the present work, the efficient fluorescence quenching of the D band and the lack of vibrational structure beyond 360 $cm^{-1}$, observed by Chin et al.,[9] is closely related to the absence of lines from the other 9-AH-G rotamer in R2PI and UV spectra. In the excited state, a rather shallow barrier separates the $RN_7$ minimum from the potential well of the $RN_1$ rotamer where a fast nonradiative decay to the electronic ground state occurs.

**Acknowledgment.** Financial support for this work from the German Research Council DFG (Grant No. SFB 663/C1) is gratefully acknowledged. I would like to thank K. Kleinermanns, M. Schmitt, and R. Weinkauf (Düsseldorf) for many stimulating discussions as well as Hans Ågren and his group for their warm hospitality during my sabbatical stay at the Royal Institute of Technology in Stockholm.

**Supporting Information Available:** Optimized minimum geometries and nuclear arrangements at conical intersections of eight guanine tautomers 9H-1H-AO-G, 7H-1H-AO-G, 9H-AH-G ($RN_1$), 9H-AH-G ($RN_7$), 7H-AH-G ($RN_1$), 7H-1H-3H-IO-G (Z), 7H-1H-3H-IO-G (E), and 7H-3H-AO-G and complete ref 21. This material is available free of charge via the Internet at http://pubs.acs.org.

## References and Notes

(1) Crespo-Hernández, C. E.; Cohen, B.; Hare, P. M.; Kohler, B. *Chem. Rev.* **2004**, *104*, 1977−2019.
(2) Kang, H.; Lee, K. T.; Jung, B.; Ko, Y. J; Kim, S. K. *J. Am. Chem. Soc.* **2002**, *124*, 12958−12959.
(3) Canuel, C.; Mons, M.; Piuzzi, F.; Tardivel, B.; Dimicoli, I.; Elhanine, M. *J. Chem. Phys.* **2005**, *122*, 074316.
(4) Nir, E.; Grace, L.; Brauer, B.; de Vries, M. S. *J. Am. Chem. Soc.* **1999**, *121*, 4896−4897.
(5) Nir, E.; Janzen, C.; Imhof, P.; Kleinermanns, K.; de Vries, M. S. *J. Chem. Phys.* **2001**, *115*, 4604−4611.
(6) Piuzzi, F.; Mons, M.; Dimicoli, I.; Tardivel, B; Zhao, Q. *Chem. Phys.* **2001**, *270*, 205−214.
(7) Mons, M.; Dimicoli, I.; Piuzzi, F.; Tardivel, B.; Elhanine, M. *J. Phys. Chem. A* **2002**, *106*, 5088−5094.
(8) Nir, E.; Plützer, C.; Kleinermanns, K.; de Vries, M. *Eur. Phys. J. D* **2002**, *20*, 317−329.
(9) Chin, W.; Mons, M.; Dimicoli, I.; Piuzzi, F.; Tardivel, B; Elhanine, M. *Eur. Phys. J. D* **2002**, *20*, 347−355.
(10) Nir, E.; Kleinermanns, K.; Grace, L.; de Vries, M. S. *J. Phys. Chem. A* **2001**, *105*, 5106−5110.
(11) Nir, E.; Hünig, I.; Kleinermanns, K.; de Vries, M. S. *Chem. Phys. Chem.* **2004**, *5*, 131−137.
(12) Choi, M. Y.; Miller, R.E. *J. Am. Chem. Soc.* **2006**, *128*, 7320−7328.
(13) Marian, C. M. *J. Chem. Phys.* **2005**, *122*, 104314.
(14) Seefeld, K. A.; Plützer, C.; Löwenich, D.; Häber, T.; Linder, R.; Kleinermanns, K.; Tatchen, J.; Marian, C. M. *Phys. Chem. Chem. Phys.* **2005**, *7*, 3021−3026.
(15) Mons, M.; Piuzzi, F.; Dimicoli, I.; Gorb, L.; Leszczynski, J. *J. Phys. Chem. A* **2006**, *110*, 10921−10924.
(16) Shukla, M. K.; Leszczynski, J. *Chem. Phys. Lett.* **2006**, *429*, 261−265.
(17) Chen, H.; Li, S. *J. Phys. Chem. A* **2006**, *110*, 12360−12362.
(18) Lee, C. T.; Yang, W. T; Parr, R. G. *Phys. Rev. B* **1988**, *37*, 785−789.
(19) Becke, A. D. *J. Chem. Phys.* **1993**, *98*, 5648−5652.
(20) Stephens, P. J.; Devlin, F. J.; Chabalowski, C. F.; Frisch, M. J. *J. Phys. Chem.* **1994**, *98*, 11623−11627.
(21) Ahlrichs, R. *Turbomole*, version 5.6; Universität Karlsruhe: Germany, 2002.
(22) Furche F.; Ahlrichs, R. *J. Chem. Phys.* **2002**, *117*, 7433−7447.
(23) Neugebauer, J.; Reiher, M.; Kind, C.; Hess, B. A. *J. Comp. Chem.* **2002**, *23*, 895−910.
(24) Scott A. P.; Radom, L. *J. Phys. Chem.* **1996**, *100*, 16502−16513.
(25) Grimme, S.; Waletzke, M. *J. Chem. Phys.* **1999**, *111*, 5645−5655.
(26) Schäfer, A.; Huber, C.; Ahlrichs, R. *J. Chem. Phys.* **1994**, *100*, 5829−5835.
(27) Weigend, F.; Häser, M.; Patzelt, H.; Ahlrichs R. *Chem. Phys. Lett.* **1998**, *294*, 143−152.
(28) Schaftenaar, G.; Noordik, J. H. *J. Comput.-Aid. Mol. Des.* **2000**, *14*, 123−134.
(29) Piacenza, M.; Grimme S. *J. Comp. Chem.* **2003**, *25*, 83−98.
(30) Hanus, M.; Ryjáček, F.; Kabeláč, M.; Kubař, T.; Bogdan, T. V.; Trygubenko, S. A.; Hobza, P. *J. Am. Chem. Soc.* **2003**, *125*, 7678−5688.
(31) Langer, H; Doltsinis, N. L. *J. Chem. Phys.* **2003**, *118*, 5400−5407.

(32) Shukla, M. K.; Leszczynski J. *J. Phys. Chem. A* **2005**, *109*, 7775−7780.
(33) Wang, S.; Schaefer, H. F., III. *J. Chem. Phys.* **2006**, *124*, 044303.
(34) Chen, H.; Li, S. *J. Chem. Phys.* **2006**, *124*, 154315.
(35) Mennucci, B.; Toniolo, A.; Tomasi, J. *J. Phys. Chem. A* **2001**, *105*, 7126−7134.
(36) Harmonic vibrational frequencies could not be determined in the Rydberg potential well for technical reasons. Typically, ZVPE corrections are smaller in the excited state.
(37) Chin, W.; Mons, M.; Piuzzi, F.; Tardivel, B; Dimicoli, I.; Gorb, L.; Leszczynski, J. *J. Phys. Chem. A* **2004**, *108*, 8237−8243.
(38) Perun, S.; Sobolewski, A. L.; Domcke, W. *J. Am. Chem. Soc.* **2005**, *127*, 6257−6265.
(39) Chen, H.; Li, S. *J. Phys. Chem. A* **2005**, *109*, 8443−8446.
(40) Blancafort, L. *J. Am. Chem. Soc.* **2006**, *128*, 210−219.
(41) Serrano-Andrés, L.; Merchán, M.; Borin, A. C. *Chem.−Eur. J.* **2006**, *12*, 6559−6571.
(42) Serrano-Andrés, L.; Merchán, M.; Borin, A. C. *Proc. Natl. Am. Soc.* **2006**, *103*, 8691−8696.
(43) Perun, S.; Sobolewski, A. L.; Domcke, W. *Mol. Phys.* **2006**, *104*, 1113−1121.
(44) Marian, C. M. To be published.